Investigating the Inline Design Measure in Existing Pressurized Steel Piping Systems

Mohamed Fersi[1(✉)] and Ali Triki[2]

[1] Department of Mechanics, National Engineering School of Sfax, University of SFAX, B.P. 1173, 3038 Sfax, Tunisia
mohamedfersi@yahoo.com
[2] Research Unit: Mechanics, Modelling Energy and Materials M2EM, National Engineering School of Sfax, University of SFAX, Sfax, Tunisia
ali.triki@enis.rnu.tn

Abstract. This paper examined the effectiveness of the inline re-design strategy used to mitigate the cavitating flow into an existing steel piping system. This strategy is based on substituting a short-section of the transient sensitive region of the existing main pipe by another one made of (**HDPE**) or (**LDPE**) plastic material. The (**1−D**) pressurized pipe flow model based on the Ramos formulation was used to describe the flow behavior, along with the fixed grid Method of Characteristics being used for numerical computations. From the case studied, it was shown that such a technique could mitigate the undesirable cavitating flow onset. Besides, this strategy allowed positive-surge magnitude attenuation. It was also found that pressure rise or drop attenuation was slightly more important for the case using an (**LDPE**) inline plastic short-section than that using an (**HDPE**) one. Furthermore, results evidenced that other factors influencing the surge attenuation rate were related to the short-section dimensions.

Keywords: Design · **HDPE** · **LDPE** · Method of characteristics · Plastic material · Ramos formulation · Viscoelasticity · Water-Hammer

1 Introduction

Water-hammer is a common phenomenon that hydraulic designers and engineers have to face in pressurized piping systems. This phenomenon generates pressure–rise and-drop and even sub-atmospheric pressure, which can produce the collapse of the system depending on the conditions of the installation.

Among the various available classical design tools taken to control water-hammer surges, we distinguish: (i) the "passive measures", which are based on the selection of pipe-wall material, pressure classes and thicknesses, according to the ultimate allowable transient pressure. Albeit, this alternative allows good hydraulic performances, it may significantly increase the cost of the piping systems, if used separately; (ii) the "active measures" which influences the operational procedures of the system by equipping the hydraulic systems with protective devices to absorb excessive pressure rise or drop [3, 12, 14, 21, 24]. Aside from the analysis of the used technologies in the

N. Aifaoui et al. (Eds.): CMSM 2019, LNME, pp. 74–82, 2020.
https://doi.org/10.1007/978-3-030-27146-6_9

available protective devices, it must be delineated that none of these technologies is a panacea that can be used inherently for all piping system; the adequate protective strategy is specific for each system case and depends upon the initiating transient event type. Oftentimes, a combination of multiple devices may prove to be the most desirable [22]. Nonetheless, this method exhibits some drawbacks arising from technical implementation constraints and the requirement of system shutdowns or partial load operation of hydraulic machineries ([16, 20]). In addition, due to the complex nature of the transient behavior, a device intended to attenuate a transient condition could even result in the worsening of another condition if the device is not adequately selected and/or located in the system [15].

In this regards, several researches (e.g.: Ghilardi et al. [7–9, 15–20]) addressed the inline-based design strategy, in order to address the forgoing drawbacks. Namely, the authors examined the efficiency of adding a plastic short-section in-line to the sensitive region of the original piping system (or substituting a short-section of the sensitive region of existing steel-piping system by another one made of plastic material) to attenuate both positive and negative hydraulic-head surge. The authors observed that the employed plastic short-section reduced the first pressure-surge peak and crest. Nonetheless, the authors noticed increasingly effect of pressure-wave oscillations period into the protected piping system; which may have adverse effect on the operational procedure of the hydraulic system. Physically, this result is attributed to the viscoelastic behavior of plastic materials which have a retarded deformation component in addition to the immediate one, observed in the case of elastic materials [1, 4, 6, 11, 25].

Considering the aforementioned discussion, the main intention of this paper is to explore the efficiency of the inline strategy to mitigate a cavitating flow onset induced into an existing steel piping system. Special focus is given for the hydraulic-head attenuation rate and the wave oscillation period spreading effects.

The next section outlines the numerical procedure used for solving the transient flow problem.

2 Materials and Methods

According to Ramos et al. [13], the one dimensional (**1−D**) transient flow equations accounting for pipe-wall viscoelasticity and unsteady friction effects, may be expressed as follows:

$$\frac{\partial H}{\partial t} + \frac{a_0^2}{gA}\frac{\partial Q}{\partial x} = 0 \tag{1}$$

$$\frac{1}{A}\frac{\partial Q}{\partial t} + g\frac{\partial H}{\partial x} + g\left(h_{f_s} + \frac{1}{gA}\left(k_{r1}\frac{\partial Q}{\partial t} + k_{r2}a_0\, Sgn(Q)\left|\frac{\partial Q}{\partial x}\right|\right)\right) = 0 \tag{2}$$

where, H is the hydraulic-head; Q is the flow discharge; A is the cross sectional area of the pipe; g is the gravity acceleration; a_0 is the wave speed; x and t are the longitudinal coordinate along the pipeline axis and the time, respectively; the quasi-steady head loss

component per unit length h_{f_s} is computed for turbulent and laminar flow, respectively, as follows: $h_{f_s} = RQ|Q|$ and $h_{f_s} = 32\nu Q/(gD^2A)$ where, $R = f/(2DA)$ is the pipe resistance; ν is the Poisson ratio; $k_{r1} = 0.003$ and $k_{r2} = 0.04$ are two decay coefficients [13].

The numerical solution of momentum and continuity Eqs. (1) and (2), within a multi-pipe system framework, is typically performed using the Fixed-Grid Method of Characteristics (**FG-MOC**) [5, 8, 10, 13, 15, 19].

Briefly, the compatibility equations, corresponding to the finite difference discretization of Eqs. (1) and (2) along the set of characteristic lines of the computational grid, may be expressed as follows:

$$\mathbf{C}_{\pm}^{j}: \frac{dQ^j}{dt} + \frac{gA^j}{\alpha^{\pm} \times (1+k_{r1})}\frac{dH^j}{dt} + \frac{f^j}{2d^j(1+k_{r1})}Q^j\left|Q^j\right| = 0 \text{ along } \frac{dx^j}{dt} = \alpha_{\pm}^{j} \tag{3}$$

where,

$$\alpha_{\pm}^{j} = 2a_0^j(1+k_{r1}) \Big/ \left(-\mathbf{Sgn}\left(Q\frac{\partial Q}{\partial x}\right)k_{r2} \pm (2+k_{r1})\right).$$

The relationships between the hydraulic-head and discharge parameters along the characteristics lines may be deduced directly from Eq. (3) as follows:

$$\begin{cases} \mathbf{C}_{+}^{j} : Q_{i,t}^{j} = c_p^{\prime j} - c_p^{\prime\prime j} H_{i,t}^{j} \\ \mathbf{C}_{-}^{j} : Q_{i,t}^{j} = C_n^{\prime j} + c_n^{\prime\prime j} H_{i,t}^{j} \end{cases} \tag{4}$$

in which: $c_p^{\prime j} = Q_{i-1,t-1}^{j} + c_p^{\prime\prime j} H_{i-1,t-\Delta t}^{j} - c_p^{\prime\prime\prime j} \Big/ 1 + k_{r1}$; $c_p^{\prime\prime j} = gA^j/B^j\alpha_{+}^{j}$; $c_p^{\prime\prime\prime j} = \{(f^j\Delta t)/(2D^j)\}Q_{i-1,t-1}^{j}\left|Q_{i-1,t-1}^{j}\right|$; $c_n^{\prime j} = Q_{i+1,t-1}^{j} + c_n^{\prime\prime j} H_{i+1,t-\Delta t}^{j} + c_p^{\prime\prime\prime j} \Big/ 1 + k_{r1}$; $c_n^{\prime\prime j} = gA^j/B^j\alpha_{-}^{j}$; $c_n^{\prime\prime\prime j} = \{(f^j\Delta t)/(2D^j)\}Q_{i+1,t-1}^{j}\left|Q_{i+1,t-1}^{j}\right|$; $B^j = gA^j/a_0^j$; the indices i denotes the section index of the jth pipe $\left(1 \le i \le n_s^j\right)$; n_s^j designates the number of sections of the jth pipe, respectively; the indices $i \pm 1$ refer to the characteristics nodes, in the characteristics grid, at the left and right sides of node i; Δt and Δx correspond to the time and space-step increments, respectively.

The numerical procedure, outlined above, allows hydraulic parameters computation, for a single-phase flow. For the cavitating flow onset, the discrete gas cavity model (**DGCM**) may be included in the (**MOC**) procedure assuming that cavities are lumped at the computing sections [10, 26, 27].

Using the perfect gas law, the isothermic evolution of each isolated gas cavity can be written as:

$$\forall_{gi}^{t}\left(H_i^t - z_i - H_v\right) = (H_0 - z_i - H_v)\alpha_0 A\Delta t \tag{5}$$

where H_0 is the reference piezometric-head; α_0 the void fraction at H_0; z_i the pipe elevation; and H_v the gauge vapor hydraulic-head of the liquid.

The equation calculating cavity volume $\forall_g$, at a given cross-section, is derived from the discretization of local continuity equation using the **FG-MOC**:

$$\forall_{gi}^{t} = \forall_{gi}^{t-2\Delta t} + \left[\psi\left(Q_i^t - Q_{ui}^t\right) - (1-\psi)\left(Q_i^{t-2\Delta t} - Q_{ui}^{t-2\Delta t}\right)\right]2\Delta t \tag{6}$$

where, $\forall_{gi}$ and $\forall_{gi}^{t-2\Delta t}$ correspond to the cavity volumes at the current time step and at $2\Delta t$ time steps earlier, respectively, and ψ is a weighting factor, chosen in the range: $0.5 \leq \psi \leq 1$ [2].

It is worth noting that the cavity collapses inasmuch as $\forall_g \prec 0$. In this case, and hence, the liquid phase is re-established and the one-phase water-hammer solver is valid again.

Series Junction

A common hydraulic grade-line elevation and no flow storage assumptions are made for calculating the flow parameters at the series section [15, 17, 23].

$$Q_{ns^j,t}^{j-1} = Q_{1,t}^{j} \text{ and } Q_{ns^j,t}^{j-1} = Q_{1,t}^{j} \tag{7}$$

where, the right and left hands of Eq. (7) correspond to the hydraulic parameters estimated at the up- and down-stream sides of the junction.

3 Application, Results and Discussion

The original hydraulic system layout, considered in this study, consists of a sloping pipe system connecting two pressurized tanks and equipped with a ball valve at its inlet. The main steel pipeline characteristics are: $E_0^{\mathbf{steel}} = 210$ GPa; $D = 44.1$ mm; $L = 100$ m; and $a_0 = 1302.5$ m/s. The downstream pipe axis is taken as the horizontal datum level ($z_d = 0$ m) and the upstream reservoir level is $z_u = 2.03$ m. The gauge saturated hydraulic-head of the liquid is equal to: $H_g = -10.2$ m. The initial steady-state regime was established for a constant flow velocity a static hydraulic-head values set equal to $V_0 = 1.04$ m/s and $H_0^{T_2} = 21.4$ m, respectively; prior to a transient event corresponding to the fast and full closure of the upstream valve. The boundary conditions associated with such an event may be expressed as follows.

$$Q_{|x=0} = 0 \text{ and } H_{|x=L} = H_0^{T_2} \ (t \succ 0) \tag{8}$$

In such a situation, the inline technique consists in substituting an upstream short-section of the main steel pipe by another one made of plastic pipe-wall material (Fig. 1).

As a starting step, the inline plastic short-section length and diameter are selected equal to: $l_{\text{short-section}}^{\text{plastic}} = 5$ m and $d_{\text{short-section}}^{\text{plastic}} = 50.6$ mm, respectively.

The input parameters of the **FG-MOC** embedding the **DGCM** procedure are: time step $\Delta t = 0.034\,\text{s}$; Courant numbers $c_{\text{r}}^{\text{steel-pipe}} = 0.9841$ and $c_{\text{r}}^{\text{plastic short-section}} = 1$, corresponding to the main steel-pipe and the plastic short-section; and $\psi = 0.5$.

Figure 2 compares the upstream hydraulic-head signals, versus time, involved by the hydraulic systems with and without applying the inline technique. Jointly, the main features of the wave curves, plotted in Fig. 2, are enumerated in Table 1.

As can be seen from Fig. 2, such a transient event leads to the occurrence of the unfavorable cavitation phenomenon, into the original system case. However, if instead a plastic short-section inline technique is implemented, the cavitation phenomenon may be palliated.

A detailed analysis of Fig. 2 and Table 1 reveals that, for the original system case, the change in the upstream boundary condition triggered a series of positive and negative surge waves. In addition, the hydraulic-head profile, corresponding to this case, illustrates a short-duration pulses resulting from the superposition of surge wave involved by the valve-closure and the wave generated by the collapse of the vapor cavity. Besides, this hydraulic-head pulses exhibit a downward gradual attenuated trend due to friction losses.

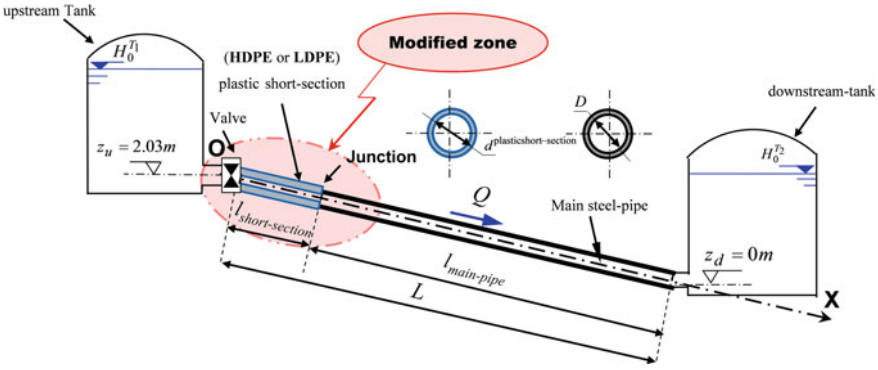

Fig. 1 Definition sketch of the hydraulic system

Basing on Fig. 2, the hydraulic-head fluctuations are characterized by a drop to the saturated hydraulic-head of the liquid ($H_{\text{min}}^{\textbf{Steel pipe}} = -10.2$ m); followed by a subsequent pressure rise $\left(H_{\text{max}}^{\textbf{Steel pipe}} = 63.7\text{ m}\right)$. For instance, the positive and negative surge magnitudes evaluated in the original system case are equal to: $\Delta H_{\text{up-surge}}^{\textbf{Steel pipe}} = H_{\text{max}}^{\textbf{Steel pipe}} - H_0 = 47.1$ m and $\Delta H_{\text{down-surge}}^{\textbf{Steel pipe}} = H_0 - H_{\text{min}}^{\textbf{Steel pipe}} = 32.2$ m, respectively, above the initial steady-state value.

Nonetheless, analysis of the hydraulic-head signals depicted into the protected hydraulic system, shows a hydraulic-head rise or drop magnitude equal to: $\Delta H_{\text{up-surge}}^{\textbf{HDPE}} = 11.1$ m or $\Delta H_{\text{downsurge}}^{\textbf{HDPE}} = 20.9$ m for the case involving an (**HDPE**) plastic short-section (Table 1). Moreover, a lower hydraulic-head rise or drop is observed for the case involving a (**LDPE**) plastic short-section ($\Delta H_{\text{up-surge}}^{\textbf{LDPE}} = 5.4$ m or

$\Delta H^{\mathbf{HDPE}}_{\text{downsurge}} = 14.7$ m). This in return implies that the positive or negative pressure attenuation ratio obtained using a short section made of (**HDPE**) are equal to $\eta H^{\mathbf{HDPE}}_{\text{up-surge}} = \Delta H^{\mathbf{HDPE}}_{\text{up-surge}} \Big/ \Delta H^{\mathbf{steel}}_{\text{up-surge}} = 9.27\%$ or $\eta H^{\mathbf{HDPE}}_{\text{downsurge}} = \Delta H^{\mathbf{HDPE}}_{\text{downsurge}} \Big/ \Delta H^{\mathbf{steel}}_{\text{downsurge}} = 26.15\%$, respectively; and more important ratios are involved by the (**LDPE**) short-section material case (i.e.: $\eta H^{\mathbf{LDPE}}_{\text{up-surge}} = \Delta H^{\mathbf{LDPE}}_{\text{up-surge}} \Big/ \Delta H^{\mathbf{steel}}_{\text{up-surge}} = 64.91\%$ or $\eta H^{\mathbf{LDPE}}_{\text{downsurge}} = \Delta H^{\mathbf{LDPE}}_{\text{downsurge}} \Big/ \Delta H^{\mathbf{steel}}_{\text{downsurge}} = 45.65\%$, respectively).

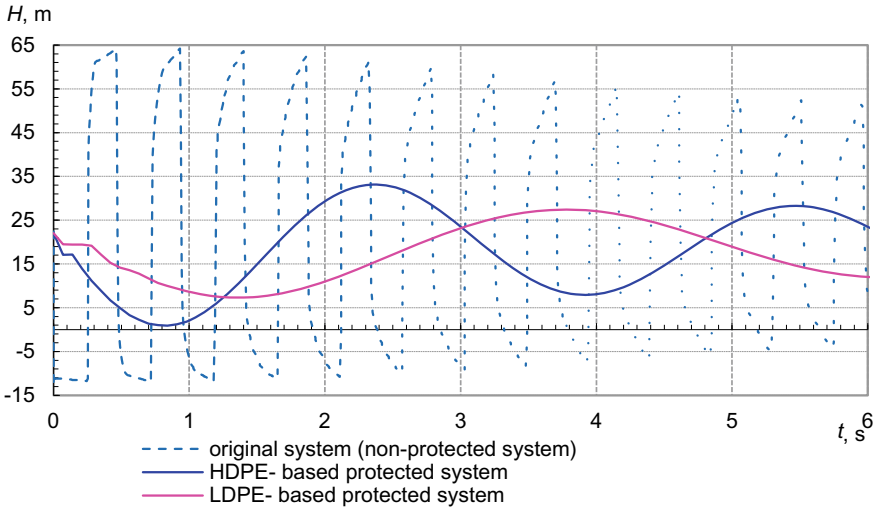

Fig. 2 Comparison of hydraulic-heads at the upstream valve section versus time for the hydraulic system with and without implementation of the protection procedure

Table 1 Characteristics of water-hammer waves in Fig. 2

Parameters		Steel main-pipe **HDPE**	Plastic short-section (**LDPE**)	
$H_{\max}$: 1st hydraulic-head peak	(m)	63.7	33.1	27.4
$H_{\min}$: 1st hydraulic-head crest	(m)	−10.2	1.1	7.3
T_1: period of the 1st cycle of wave oscillation	(s)	0.41	1.37	3.73

On the other side, based on Fig. 2 and Table 1, it is remarkable to point out that the periods of the first cycle of hydraulic-head oscillations, predicted into a (**HDPE**) or (**LDPE**) plastic short-section-based protected system case are: $T_1^{\mathbf{HDPE}-\text{penstock}} = 1.37$ s or $T_1^{\mathbf{LDPE}-\text{penstock}} = 3.37$ s; while the corresponding period associated with the original

system case is equal to $T_1^{\mathbf{steel-pipe}} = 0.41$ s. Thereupon, the inline technique based on a (**HDPE**) or (**LDPE**) short-section induces a spreading of the wave oscillations period equal to: $\delta T^1_{\mathbf{HDPE}} = \left|T^1_{\mathbf{steel}} - T^1_{\mathbf{HDPE}}\right| = |0.41 - 1.37| = 0.96$ s or $\delta T^1_{\mathbf{LDPE}} = \left|T^1_{\mathbf{steel}} - T^1_{\mathbf{LDPE}}\right| = |0.41 - 3.73| = 3.32$ s as compared with that involved by the original system case. Furthermore, the period spreading induced by the (**LDPE**) short-section–based inline technique relatively to the **HDPE** short-section–based inline technique is equal to: $\delta' T^1_{\mathbf{LDPE}} = \left|T^1_{\mathbf{HDPE}} - T^1_{\mathbf{LDPE}}\right| = 3.73 - 1.37 = 2.36$ s).

The preceding discussions argue that the (**HDPE**)-based inline technique allows better trade-off, between the attenuation of hydraulic-head peak (and crest) and the limitation of spreading of hydraulic-head oscillation period, as compared with the (**LDPE**)-based one.

All the results presented thus far were obtained for a specific short-section size (i.e.: $d^{\text{plastic}}_{\text{short-section}} = 50.6$ mm and $l^{\text{plastic}}_{\text{short-section}} = 5$ m). Additional results with respect to the magnitude sensitivity of the first hydraulic-head crest to the size of the replaced plastic short-section are reported in Fig. 3a and b, for several diameter and length values of the employed short-section: $d^{\text{plastic}}_{\text{short-section}} = \{45; 50.6; 75 \text{ and } 100 \text{ mm}\}$ and $l^{\text{plastic}}_{\text{short-section}} = \{5;\ 7.5;\ 10;\ 12.5 \text{and } 15 \text{ m}\}$, respectively.

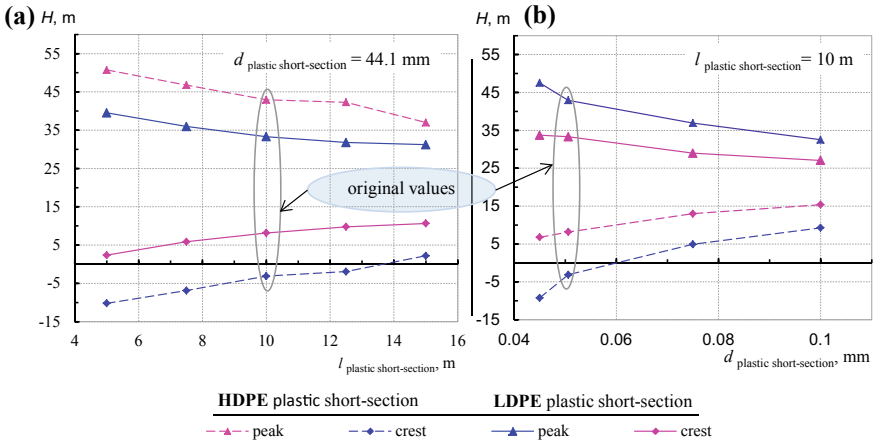

Fig. 3 Variation of hydraulic-head peaks and crests at the downstream valve section depending on the plastic short-section: **a**—length, **b**—diameter

Figure 3a and b suggest that for length and diameter values beyond $l^{\text{plastic}}_{\text{short-section}} \geq 10$ m and $d^{\text{plastic}}_{\text{short-section}} \geq 44.1$ mm, respectively, the variation of the first transient pressure crests is slightly affected. Consequently, the diameter value $d^{\text{plastic}}_{\text{short-section}} = 44.1$ mm and the length value $l_{\text{short-section}} = 10$ m may be considered as the optimal values of the plastic short-section size for the case studied herein.

4 Conclusion

In summary, the present study highlighted that the employed technique provides a large damping of the first pressure peak and crest associated to a transient initiating event. In addition, this pressure damping is observed to be more pronounced when using a (**LDPE**) plastic material for the added short-section than an (**HDPE**) material. However the former technique induces more important wave period spreading as compared with the latter one. Furthermore, it is also shown that other factors contributing to the hydraulic-head attenuation rate depend upon the short-section size (i.e. length and diameter). Specifically, examination of the sensitivity of the pressure peak or crest magnitude, with the short-section length and diameter being the controlling variables, verifies that significant volumes of the short-section provide important hydraulic-head attenuation. However, this correlation is not significant beyond a near-optimum diameter and length values.

One intends that such a technique may greatly enhance the reliability and improve the cost-effectiveness of industrial hydraulic utilities, while safeguarding operators. Future test configurations including pipe networks may represent an extension to this study.

References

1. Aklonis JJ, MacKnight WJ, Shen M (1972) Introduction to polymer viscoelasticity. Wiley-Interscience, Wiley
2. Bergant A, Simpson AR, Tijsseling A (2006) Waterhammer with column separation: a historical review. J Fluids Struct 22(2):135–171. https://doi.org/10.1016/j.jfluidstructs.2005.08.008
3. Besharat M, Tarinejad R, Ramos H (2015) The effect of water hammer on a confined air pocket towards flow energy storage system. J Water Supply Res Technol Aqua 65(2):116–126. https://doi.org/10.2166/aqua.2015.081
4. Brinson HF, Brinson LC (2008) Polymer engineering science and viscoelasticity: an introduction. Springer
5. Chaudhry MH (2014) Applied hydraulic transient. Van Nostrand Reinhold Company
6. Ferry JD (1970) Viscoelastic properties of polymers, 2nd edn. Wiley, New York
7. Fersi M, Triki A (2018) Investigation on redesigning strategies for water-hammer control in pressurized-piping systems. J Press Vessel Technol Trans ASME. https://doi.org/10.1115/1.4040136
8. Fersi M, Triki A (2019) Alternative design strategy for water-hammer control in pressurized-pipe flow. In: Fakhfakh T, Karra C, Bouaziz S, Chaari F, Haddar M (eds) Advances in acoustics and vibration II, ICAV 2018. Applied Condition Monitoring, vol 13, 135–144, Springer, pp 157–165. https://doi.org/10.1007/978-3-319-94616-0_16
9. Ghilardi P, Paoletti A (1986) Additional viscoelastic pipes as pressure surge suppressors. In: Proceedings of 5th international conference on pressure surges, Cranfield (UK), pp 113–121
10. Ghidaoui MS, Zhao M, Duncan AM, David HA (2005) A review of water-hammer theory and practice. Appl Mech Rev 58:49–76. https://doi.org/10.1115/1.1828050
11. Güney MS (1983) Water-hammer in viscoelastic pipes where cross-section parameters are time dependent. In: Proceedings of 4th international conference on pressure surges, BHRA, Bath, U.K, pp 189–209

12. Moussou P, Gibert RJ, Brasseur G, Teygeman C, Ferrari J, Rit JF (2010) Relief instability of pressure valves in water pipes. Press Vessel Technol 132(4):041308. https://doi.org/10.1115/1.4002164
13. Ramos H, Covas D, Borga A, Loureiro D (2004) Surge damping analysis in pipe systems: modelling and experiments? J Hydraul Res 42(4):413–425. https://doi.org/10.1080/00221686.2004.9641209
14. Rosselló JM, Urteaga R, Bonetto FJ (2018) A novel water hammer device designed to produce controlled bubble collapses. Exp Therm Fluid Sci 92:46–55. https://doi.org/10.1016/j.expthermflusci.2017.11.016
15. Triki A (2016) Water-hammer control in pressurized-pipe flow using an in-line polymeric short-section. Acta Mech 227(3):777–793. https://doi.org/10.1007/s00707-015-1493-13
16. Triki A (2017) Water-Hammer control in pressurized-pipe flow using a branched polymeric penstock. J Pip Syst Eng Pract ASCE 8(4):04017024. https://doi.org/10.1061/(ASCE)PS.1949-1204.0000277
17. Triki A (2018) Further investigation on water-hammer control inline strategy in water-supply systems. J Water Suppl Res Technol AQUA 67(1): 30–43. https://doi.org/10.2166/aqua.2017.073
18. Triki A (2018) Dual-technique based inline design strategy for Water-Hammer control in pressurized-pipe flow. Acta Mech 229(5):2019–2039. https://doi.org/10.1007/s00707-017-2085-z
19. Triki A, Fersi M (2018) Further investigation on the Water-Hammer control branching strategy in pressurized steel-piping systems. Int J Press Vessels Pip 165(C):135–144. https://doi.org/10.1016/j.ijpvp.2018.06.002
20. Triki A, Chaker MA (2019) Compound technique -based inline design strategy for water-hammer control in steel pressurized-piping systems. Int J Press Vessel Pip 169C:188–203. https://doi.org/10.1016/j.ijpvp.2018.12.001
21. Wan W, Huang W (2011) Investigation on complete characteristics and hydraulic transient of centrifugal pump. J Mech Sci Technol 25:2583. https://doi.org/10.1007/s12206-011-0729-9
22. Wan W, Li F (2016) Sensitivity analysis of operational time differences for a pump-valve system on a water hammer response. J Press Vessel Technol Trans ASME 138(1):011303. https://doi.org/10.1115/1.4031202
23. Wan W, Huang W (2018) Water hammer simulation of a series pipe system using the MacCormack time marching scheme. Acta Mech 229(7):3143–3160 https://doi.org/10.1007/s00707-018-2179-2
24. Wan W, Zhang B (2018) Investigation of water hammer protection in water supply pipeline systems using an intelligent self-controlled surge tank. Energies 11(6):1450. https://doi.org/10.3390/en11061450
25. Weinerowska-Bords K (2006) Viscoelastic model of waterhammer in single pipeline—problems and questions. Arch Hydro-Eng Environ Mech 53(4):331–351. ISSN 1231–3726
26. Wylie EB, Streeter VL (1993) Fluid transients in systems. Prentice Hall, Englewood Cliffs, NJ
27. Zang B, Wan W, Shi M (2018) Experimental and numerical simulation of water hammer in gravitational pipe flow with continuous air entrainment. Water 10(7):928. https://doi.org/10.3390/w10070928